

General Report: Session 1B on Physical and Constitutive Modelling

Vincenzo Fioravante & Daniela Giretti
The University of Ferrara, Engineering Department, Italy

ABSTRACT

This report drives a path through some of the main issues discussed by the 84 papers presented to the Session 1B – on Physical and Constitutive Modelling – of the 17th ICSMGE and evidences some of the results of major interest, with the aim of outlining the role of modelling in geotechnical engineering. *Physical, theoretical/constitutive* and *numerical* modelling strongly interact in design practice. Design is usually undertaken via simple conceptual models or rigorous numerical analyses; physical modelling provides important benchmarks for calibrate conceptual models and to validate numerical analyses and is particular useful when dealing with complex geotechnical problems.

Keywords : physical modelling, constitutive modelling, numerical analyses

1 INTRODUCTION ON MODELLING

According to Muir Wood 2004: “...almost everything that engineers do is concerned with modelling”. A model is an appropriate simplification of reality and engineering is fundamentally concerned with identifying the key features needed to be accounted in the design and to be modelled, to solve a real problem.

A schematic description of models is here reported.

Empirical models

Many of the geotechnical engineering techniques are based on experiences (empiricism), on procedures that can provide satisfactory answers even though the mathematical formulation cannot be justified in a more general mechanical framework (inductive models).

Physical models

Every experiment can be considered a physical model, directed to confirm or develop theoretical/empirical assumptions; the features of the actual engineering problem to be analysed (prototype) are reproduced (model) and tested to study the behaviour of the prototype. The term “physical modelling” is habitually associated with the performance of physical testing of complete geotechnical systems in which the real geotechnical materials are used.

Full scale models: all features of the prototype being studied are reproduced at full scale; they are employed when the behaviour of the prototype is so dependent on the detail of actual soil fabric and structure. Trial embankments on soft soils provide an example, when used to evaluate process of ground improvement or time dependent behaviour (creep settlements).

Small scale models: Most of physical models are constructed at much smaller scale than the prototype because it is desired to obtain information about expected patterns of response more rapidly and with closer control over model details than would be possible with full scale testing and since the model can experience limit conditions until failure is reached. The key question is concerned with establishing the validity of the models and ensuring a secure way to extrapolate the observations made at small scale to the prototype scale (scaling laws).

Conceptual models

Theoretical models: the engineering problem is described with a formulation included in a framework of general validity (deductive models). There are two possible applications of theoretical modelling: either the boundary conditions of the problem can be well established in such a way that an exact analytical closed-form solution can be obtained or a numerical formulation is required with adequate approximations. Exact, closed-form solutions are in general accessible for a limited set of conditions.

Constitutive models: link between stress and strain changes; the idealisation of material behaviour is necessary in order that simple theoretical models can be developed. Linearity is generally associated with elasticity while non linearity observed in soil behaviour is associated with plasticity, permanent, irrecoverable changes in the fabric of the soil; time-dependent deformation can be associated with visco-plasticity. A constitutive model is a simplification of soil behaviour, is based on experimental observation and its parameters are generally calibrated via laboratory tests; it takes into account the features of soil behaviour of major interest for a specific application.

Semi-empirical models: simplified correlations founded partially on theoretical model and partially on experimental results (deductive and inductive models at the same time).

Numerical models

If an engineering problem can not be fitted to one of the limited sets of the exact solutions and its distance from the ideal situation is too great, there is the possibility of using numerical techniques to obtain a solution, using the numerical approximation to allow realistic boundary conditions to be accommodated. Numerical simulation usually implies the replacement of continuous description of a problem by one in which the solution is only obtained at a finite number of points in space and times. The quality of the numerical modelling result can only be as good as the quality of the numerical approximation. Numerical modelling is needed to manage irregular or non-ideal boundary conditions.

In the geotechnical design practice, the different aspect of modelling often interplay, as outlined by Burland 1987 and Randolph & House 2001 and shown schematically in Figure 1.

Physical models are seldom used directly in the design process, more usually data from physical model tests are employed to calibrate conceptual models and to validate numerical analyses directly used for the design.

Physical and numerical modelling both require some idealisation of the real problem, and although numerical analysis computational costs are lower than physical modelling charge, for the understanding of complex geotechnical engineering problems physical modelling represents the actual most powerful research tool.

Conceptual models can be developed from observation of full scale and model scale data, or from results of numerical analyses.

Data from monitoring of actual structures can be advantageously used in design in combination with physical tests or numerical analysis results.

This General Report, moving through the papers allocated in the Session 1b of the Conference, focuses on the role of modelling in geotechnical engineering and on the principal engineering applications of modelling. Due to the very large number of topics treated by the 84 papers presented, only some of the main applications are briefly recalled some of those considered interesting to stimulate the floor discussion.

The design problems which have been investigated by means of conceptual, numerical and physical modelling in Session 1b include large deformations or interaction within the soil medium problems (e.g. retaining walls, capacity of piles, soil improvement, performance of embedded drag anchors, effects of sand piles and jet grouting); creep or secondary consolidation phenomena (e.g. reinforced embankment); cyclic and dynamic loading effects (e.g. earthquake induced liquefaction or residual displacement, offshore foundations); transport process within the soil (e.g. seepage, subsurface erosion and contaminated sites); complex soil response (e.g. non-linear soil behaviour, anisotropy, rate and strain dependent behaviour).

2 LIST OF PAPERS

Table 1, lists the papers presented in Session 1B, on physical and constitutive modelling, and provides a succinct description of the topics discussed. All the models presented have been classified in: physical models (1g, laboratory and ng),

theoretical/constitutive models, semi-empirical correlations and numerical analyses.

The main engineering applications of the modelling examples described in the communications have been subdivided in five groups, defined in the second column of Table 1 by a letter, from a to e, where:

- a = mechanics of soil, rock and composite materials, 39 papers presented
 - b = onshore, offshore and “extraterrestrial”, shallow and deep foundations, 15 papers
 - c = slope stability, earth pressure and retaining structures, 10 papers
 - d = embankments and ground improvement, 15 papers
 - e = tunnelling, 5 papers
- 6 papers, marked with a (*), deal with dynamic conditions.

Very often physical model tests have been interpreted using image analyser techniques, which are widely considered very powerful tools to analyse the behaviour of the whole system tested (e.g. deformations patterns, kinematics interactions, failure mechanisms).

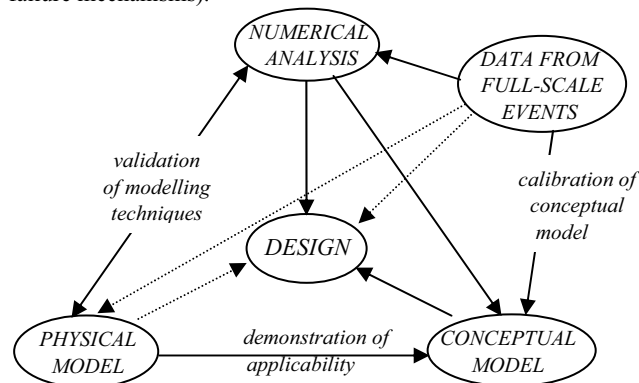


Figure 1: Interaction of different aspects of modelling in design (Randolph and House, 2001)

Table 1. List of papers of Session 1b.

PHYSICAL MODELS – 1g small scale & laboratory

N.		Title	Authors	Topics
1	c	Experimental study of the pullout resistance of ribbed anchors in sands	Irsyam, Hasan Hryciw	Experimental study into the pullout resistance of smooth, rough, and ribbed cylindrical anchor in dense and loose sands performed in a large triaxial testing tank at various confining pressures
2	a	A model experiment to asses the effects of inclusions on wave propagation in soil media	Houston & Ray	Data acquisition system using Micro-Electro-Mechanical Systems (MEMS) technology for data collection of changes of wave propagation caused by inclusions in a uniform media; experimental results from 5m square test pit
3	c, d	Physical and numerical modeling of shear band formation	Katzenbach Bachmann Gutberlet	Model tests and numerical results for the examination of shear band formation in homogenous and stratified soil concerning earth pressure, base and slope failure
4	d	Monitoring soil stiffness gain due to lateral preloading	Biringen Fratta & Edil	Experiment to evaluate the effect of lateral loading on stiffness and strength improvement of foundation soils with close-ended cylindrical piles
5	a	Partitioning tracer test for monitoring petroleum contamination in subsurface; 3D sand box experiment	Rhee & Park	Partitioning tracer test conducted in a three-dimensional sand box before and after containing a petroleum spill to test the validity of the proposed method in real groundwater flow
6	d	Model tests and PIV analysis on failure behaviour of embankment due to injected water	Nakata Murata & Orense	Collapse mechanisms of an embankment slope as a result of water injection; application of particle image velocimetry to analyse failure pattern
7	b	Experimental study of soil reaction when a rigid plate is submitted to a vertical load and a moment	Foncea & Mutoli	Variations of the coefficient of soil reaction of a clean sand placed at different relative densities under a rigid plate loaded vertically and with a monotonic moment
8	b	Load sharing under 1-g model rigid piled rafts	Türkmen & Ergun	Laboratory model tests to investigate load bearing and sharing behavior of piled raft foundations

9	<i>b</i>	The effect of sheet pile length on the capacity of sheet pile foundation	Punrattanasin, Gasaluck Muktabhant, Angsuwotai & Patjanasuntorn	Effects of sheet pile length on improving the vertical, horizontal and moment capacities of existing shallow foundations; image processing technique used to identify the mode of failure and to calculate the soil movement and displacement vector below the foundation
10	<i>d</i>	Variation of soil density and earth pressure due to strip compaction	Fang Chien	Variation of soil density and earth pressure in a soil mass due to the vibratory compaction along a strip on the surface of a cohesionless backfill
11	<i>b</i>	Shaking table tests on model piles in liquefiable sand	Ueng, Chen & Tseng	Lateral load and shaking table tests in a large biaxial laminar shear box filled with saturated sand of various densities for the study of the soil-pile interaction in a liquefiable soil
12	<i>d</i>	Soft soils improvement solution. Design based on the laboratory test results on scale model	Chirică, Iteanu Serbulea & Boți	Soil improvement with lime and sand piles for increasing the subgrade bearing capacity of an existing embankment; oedometer tests on samples of natural soil and soil reinforced with micro piles
13	<i>c</i>	The role of particle size in the flow behaviour of saturated granular materials	Bowman Sanvitale	Experimental research on flowing granular materials using a flume apparatus to investigate the effect of particle size distribution on the material mobility
14	<i>b</i>	Evaluation of gravity dependence of lunar surface bearing capacity	Kobayashi, Omine Suyama, Ishikura	Model tests of shallow footing systems on a simulated lunar soil in partial gravity fields reproduced on an aircraft that flew in parabolic paths
15	<i>d</i>	Soil deformation pattern in low-energy dynamic compaction	Hajjalilue-Bonab & Rezaei	Physical modelling of low energy dynamic compaction (DC) on fine dry loose sand based on image processing to derive a normalised relation between influence depth and DC parameters
16	<i>b*</i>	Dynamic impedance functions of machine foundations on sandy soils by physical model tests	Jafarzadeh & Mashhadi	Physical model tests to improve methods of design of machine foundations by means of impedance function
17	<i>e</i>	Behaviors of ground and existing structures due to circular tunneling	Shahin, Nakahara & Nagata	Relationship between surface settlement and volume loss due to shallow tunneling based on 2D model tests and the numerical analyses
18	<i>c</i>	Model tests on reinforcement effect of an anchorage work added to the existing anchored sheet pile wall	Morikawa & Kikuchi	Dual-anchored sheet pile wall reinforcement method for sheet pile wall; an additional anchorage work is attached to the existing anchored sheet pile wall to reduce the load acting on the existing wall
19	<i>c*</i>	Shaking table tests on seismic earth pressure under large earthquake loads	Watanabe & Tateyama	Shaking table tests to evaluate the seismic earth pressure on the backface of retaining wall models; comparison with Mononobe-Okebe theory
20	<i>d*</i>	Calculation method for residual displacement during earthquake for embankment affected by seepage water	Matsumaru, Kojima, Tateyama Watanabe & Watanabe	Calculation method for residual displacement during earthquake based on Newmark method, taking into consideration the effect of seepage water
21	<i>b</i>	Speckle photography for measuring 3-D deformation inside a transparent soil model	Liu, Iskander	Method for non-intrusively measuring 3D internal soil deformation, using transparent soils and laser speckle photography techniques, applied to shallow footings
22	<i>d</i>	Variation of the parameters of injection for the ground in different regimes	Farcas, Popa & Ilies	Relations between injection pressure, injection debit and periphery advance fluid velocity for one-dimensional, plan axial symmetric and spatial symmetric grouting from numerical and cylindrical wood container physical tests
23	<i>e</i>	Model tests and numerical analysis on the evaluation of long-term stability of existing tunnel	Sekine, Zhang Tasaka, Kurose & Ohmori	Failure test and constant load creep test on tunnels in a manmade soft rock model ground and FE analyses based on an elasto-visco-plastic model
24	<i>a</i>	Elasto-plastic description of mechanical behavior of silt improved by lime	Nakano & Yamada	Mechanical tests on specimens of Kira converted into pebble form by crushing and mixing with lime to study the feasible utilization of Kira sand as geomaterial and comparison with results of SYS Cam-clay model
25	<i>d</i>	Three-dimensional Large-scale test of soil-structure interface	Zhang, Hou, Feng Zhang	Large-scale test apparatus developed to investigate 3D monotonic and cyclic behaviour of soil-structure interfaces. The 3D behaviours of the gravel-steel plate interface has resulted significantly different from its two-dimensional behaviours
26	<i>a</i>	Analyse microscopique des mécanismes de dessiccation et de gonflement des sols argileux	Maison, Laouafa Delalain Fleureau	Wetting/drying cycles on two clays in the Environmental Scanning Electron Microscope chamber to understand the sensitivity of the materials to shrinkage and swelling

PHYSICAL MODELS – full scale and ng

N.		Title	Authors	Topics
1	<i>e, d</i>	Use of vertical reinforcement to reduce ground movement due to tunnelling	Juneja, Hegde & Lee	Settlement pattern due to tunnel excavation adjacent to vertical reinforcement in sand, effects of depth of the tunnel and spacing between the tunnel axis and reinforcement
2	<i>d</i>	Modeling of vibration isolation using geofoam barriers in centrifuge	Caicedo, Murillo Thorel	Efficiency of geofoam barriers on the reduction of vibrations focusing on the effect of the depth of the barrier and of the distance between vibration source and barrier

3	c	Studies on development of an innovative type sheet-pile-bulkhead	Cai, Li, Xu Liu	Tests on a new-type of sheet pile bulkhead consisting on the addition of a row of barrier piles between the front wall for retaining soil and the anchor wall, to reduce the thrust of earth pressure acting on the front wall
4	c	Investigation of the behaviour of nailed sand trenches before failure by geotechnical centrifuge	Askarinejad Shahnazari Salehzadeh	Pre-failure behaviour of loose vertical sand slopes stabilised by nailing system
5	a	Centrifuge modeling of failure patterns in mixed soil layers induced by normal faults	Hu, Cai, Luo, Ding, Dong, Hu, Hou & Ng	Investigation of ground failure patterns in sandy, silty and mixed-layer soils induced by normal bedrock fault movements during earthquakes
6	b	Plate anchor keying under inclined pullout in clay: observation and estimation	Song, Hu	Centrifuge tests on transparent soil and numerical analyses using large deformation RITSS approach to study inlined pullout of plate anchors
7	b	New centrifuge modelling techniques for investigating seabed pipeline behaviour	Gaudin & White	Newly-developed modelling techniques for simulating the dynamic laying of seabed pipelines and the effect on the as-laid pipe embedment
8	a	Study on generalized scaling law in centrifuge modeling with flat layered media	Tobita, Iai Noda	Applicability of the two stage scaling relationship (generalized scaling law) for dynamic response of flat layered media
9	c*	Evaluation of damage in geogrid reinforced soil walls based on wall displacement	Izawa Kuwano	Evaluation of damage of geogrid reinforced soil walls subjected to earthquake based on centrifuge tilting and shaking table tests
10	e*	Seismic analyses of shallow tunnels by dynamic centrifuge tests and finite elements	Bilotta, Lanzano, Russo, Silvestri Madabhushi	Tests to calibrate dynamic analyses with different approaches to account for soil-tunnel kinematic interaction
11	a*	Centrifuge model tests on soil desaturation as a liquefaction countermeasure	Takemura, Igarashi, Izawa, Okamura & Masuda	Mechanical behaviour of the submerged but partially saturated sand during earthquake to study the applicability of soil desaturation as a liquefaction countermeasure
12	a	The influence of pore pressures on penetration forces in sand and clay	Bezuijen, van Tol, Hölischer & van Lottum	Study of the rate effects on soil strength and deformation behaviour by means of penetration tests of a pile in sand and of a T-bar in clay
13	c	Monitoring of shear strain in shallow sections of slopes to detect increased risk of slope failure	Tamate & Itoh	Full-scale and centrifuge slope model tests to evaluate the efficacy of Short Pipe Strain transducer (SPS) developed to measure shear strain increments in the shallow section of slopes during cutting works
14	c	Physical modeling of slope failure during slope cutting work	Itoh, Timpong Toyosawa Tamrakar & Suemasa	Full-scale and centrifuge slope model tests to examine the mechanism of slope failure during slope cutting works

THEORETICAL and CONSTITUTIVE MODELS

N.		Title	Authors	Topics
1	a	Prediction of the onset of strain localization in non-coaxial plasticity	Huang, Lu Qian, Wang	3D non-coaxial elasto-plasticity model with a new yield function to predict strain localisation
2	a	A stress-dilatancy relation for cemented sands	Zhang Salgado	Stress-dilatancy relation for cemented sands alternative to Rowe's relation has been derived in the transformed stress space, in which the material has the same ϕ but no cohesion or tensile strength. The derivation relies on use of Rowe's saw-tooth model together with the application of the laws of friction
3	d	Dimensionnement sous sollicitation sismique de sols de fondations renforcés par inclusions rigides	Thai Son, Hassen de Buhan, Okyay Dias	Stability analysis of an embankment lying over a pile-reinforced soil subjected to a seismic loading, using a multiphase model developed in the framework of yield design and extended to elasto-plasticity
4	d	Numerical Implementation of a Viscoplastic Constitutive Equation for the Modelling of Tailings Heaps	Katzenbach Leppla & Wachter	Visco-plastic constitutive equation developed and implemented into a FE system for the modelling and simulation of the time dependent behaviour of rock salt
5	a	Numerical implementation of elasto-viscoplastic model in bituminous mixtures microstructure	Dessouky Papagiannakis & Masad	Elasto-viscoplastic continuum model to predict Bituminous Mixture response and their performance in service loading
6	a	Thermo-mechanical constitutive modeling of overconsolidated saturated clays	Hamidi & Khazaei	From modified Cam-clay model, implementing a new approach to achieve deformation formulas, a thermo-mechanical model for saturated clays is presented and validated via triaxial laboratory tests
7	a	Assessment of a viscoelastoplastic constitutive model for asphalt mix response under repeated loading	Soltani, Baziar	Visco-elasto-plastic model utilised to predict the asphalt concrete material response for a given loading history validated with the measured data from a repeated loading test
8	a	Non-linear viscous behaviour of undrained Bangkok clay	Likitlersuang & Chompoorat	Non-linear viscous behaviour of Bangkok Clay employing a rate-dependent hyperplasticity model calibrated against the undrained triaxial sheared tests
9	a	An experimental study of clay based on a class of simple hypoelastic constitutive behaviour	Vakili	Simple model based on the theory of hypoelasticity to define the mechanical behaviour of clay from the standard Triaxial (UU) test results

10	<i>a</i>	Coupled hydraulic and mechanical behavior of unsaturated soils: theory and validation	Liu Muraleetharan	A constitutive model for unsaturated sands and silts in the general stress space is presented. A hysteretic soil water characteristic curves model, a new intergranular stress, and special hardening laws are proposed to describe the coupling effects between the hydraulic and mechanical behaviour. Comparisons between model predictions and unsaturated cyclic triaxial test results on Toyoura sand are made
11	<i>a</i>	New description of stress-induced anisotropy using modified stress	Kikumoto Nakai & Kyokawa	Method for describing the influences of the intermediate principal stress and the stress histories on the deformation and the strength of soils
12	<i>b</i>	Calcul analytique des contraintes sous une plaque rigide en fonction de la nature et de l'état du sol	Ejjaaouani Shakhirev Magnan	3D stress calculation model in which the dimensions of the influence zone of a surface load are defined by a stress diffusion angle β , which depends on the nature of the soil and on some of its geotechnical characteristics, such as density and void ratio
13	<i>b</i>	Rigid plastic analysis for bearing capacity of strip footings subjected to combined loads	Kobayashi & Izawa	Rigid-plastic analysis and interactions along the interface of a footing and a soil implemented in a formulation of a hybrid type rigid plastic FEM as inequality constraint conditions
14	<i>b</i>	Bearing behaviour of shallow foundations on clays – offshore and onshore, research and practice	Hossain & Randolph	Summary of investigations undertaken to explore shallow foundation response on single and double layer clays in the context of soil flow mechanisms, cavity depth and bearing capacity
15	<i>b</i>	Stress-strain state of the system “base-strip foundation” at elimination of excessive tilts of buildings	Shokarev, Shapoval Chaplygin Samchenko Volkov	Geomechanical and design models corresponding to physical state of soil under strip foundation underworked by horizontal cylindrical boreholes to reduce construction tilting
16	<i>a</i>	Prise en compte de la non saturation dans l'interprétation de l'essai oedométrique	Boutonnier	New theory of consolidation especially developed for fine soils near saturation, applied to evaluate the instant and differed swelling after an excavation
17	<i>a</i>	Some models of soil behaviour for evaluation of consolidation settlement in clays	Rotaru Răileanu	Combination of two serial-linked distinct elements, a rheological model representing the irrecoverable deformation and a rheological model representing the recoverable deformation for evaluation of consolidation settlement in clays. The structural viscosity effects during the primary consolidation stage are evidenced
18	<i>e</i>	Simplified phase change model for artificially frozen ground subject to water seepage	Ziegler, Baier Aulbach	Phase change model to describe the unfrozen water content and the freezing behaviour as a function of the temperature. The model can be used to optimise freezing measures in the planning phase, leading to long-term cost savings

THEORETICAL CORRELATIONS

N.		Title	Authors	Topics
1	<i>a</i>	Dilatancy and shear strength behavior of sand at low confining pressures	Chakraborty & Salgado	Correlation between peak and critical-state friction angles and dilatancy based on triaxial compression and plane-strain compression test data for sand
2	<i>a</i>	The friction angle and critical state void ratio of sands	Sfriso	Modification of Bolton's dilatancy term to predict the shear strength of a sand as a function of void ratio and mean pressure using a fixed set of material parameters independent of stress state, void ratio, drainage conditions or stress path
3	<i>a</i>	Note on the shearing strength of sand	Maksimović	Hyperbolic model to describe the relationship between interparticle friction, dilatancy grain crushing, relative density and stress level at failure for sand
4	<i>a</i>	Geomechanical model for sediment profiles	Christensen Svano & Skomedal	Geomechanical model to estimate profiles of porosity and density from a minimum input of litho-stratigraphy and pressure profile. Creep plays an important role for porosity reduction in shallow sediments or deeper sediments with high porosities preserved due to overpressure
5	<i>a</i>	Behaviour of transdanubian clay under unloading and reloading	Koch	Behaviour of a common Hungarian clay via laboratory tests and determination of the input parameters for a hardening soil model for a commercial computer program
6	<i>b</i>	Impacts of plant-induced uptake on the stability of the earth structure	Kawai, Iizuka Tachibana, Ohno	Modelling the effect of vegetation-induced water uptake due to the evapotranspiration, which can induce significant differential settlement. Simulation of a real event in Poland
7	<i>a</i>	Developing a generalized multiple-step loading damage model to predict rock behaviour during multiple-step loading triaxial compression test	Taheri Tani	Generalised model developed to simulate multiple-step loading triaxial compression test to evaluate the strength parameters of rocks from a single specimen
8	<i>d</i>	Research on creep deformation of rockfill material and post-construction deformation of rockfill dam	Zeping Gang Haifang	Empirical model for creep deformation analysis of rockfill material under different conditions is developed from results of large scale stress controlled triaxial tests

9	<i>d</i>	The influence of erosion processes on the stability of permanent flood protection systems	Boley & Lenz	Calculation method to determine the critical hydraulic gradient which causes erosion of permanent flood protection systems in layered soils
10	<i>a</i>	State dependent characteristics of Bagmati sand	Jha	Pressure and density dependent characteristics of Bagmati sand using drained triaxial compression tests
11	<i>a</i>	Effects of specimen thickness and skeletal structure on consolidation behavior around consolidation yield stress	Watabe, Tanaka Sassa, Kobayashi & Udaka	Scale effect in long-term consolidation behaviour through a series of interconnected type consolidation tests

NUMERICAL ANALYSES

N.		Title	Authors	Topics
1	<i>a</i>	DEM simulation of effect of confining pressure on ballast behaviour	Thakur, Indraratna & Vinod	Discrete Element Method simulation carried out to observe the effect of confining pressure on ballast behaviour under railway environments accounting for dilatancy and particle breakage
2	<i>a</i>	Probabilistic calibration of discrete particle models for geomaterials	Medina-Cetina Khoa	Probabilistic inverse model method to calibrate numerical models based on Particle Flow Code in 3D to fully define the parameters of the particle models through a joint probability density function based on triaxial rock tests
3	<i>a</i>	Main features of two simple bond contact models for bonded granulates: PFC model and Jiang model	Jiang, Haibin Yan	Two contact bond models used in Distinct Element Method, one generates clusters of particles while the other investigates the mechanical behaviour of naturally-microstructured soils
4	<i>a</i>	Effect of particle shape and angularity on dilation of granular soils: a discrete element approach	Sallam Ashmawy	Effect of particle shape and angularity on strength and dilatancy properties of granular soils using DEM with the Overlapping Rigid Clusters method
5	<i>a</i>	Simulation of liquefaction of unsaturated sand using porous media theory	Uzuoka, Kazama Sento & Unno	Numerical simulations of unsaturated soil triaxial tests performed using the porous media theory and a simplified elasto-plastic constitutive model for sand
6	<i>a</i>	Wellbore instability mechanisms in very hard clay	Abdulhadi, Akl, Germaine & Whittle	Laboratory measurements and numerical analyses performed to understand the mechanisms of instability associated with drilling of high angle wells through un lithified mudstones/very hard clays
7	<i>a</i>	Numerical modelling for the detection and quantification of deep-ocean methane hydrates using seismics	Wojtowicz Zervos, Clayton	New numerical modelling method accounting for different hydrate morphologies within the host sediment and enhancing the existing effective medium models
8	<i>a</i>	Evaluating soil parameters using numerical optimisation	Doherty & Lehane	Mathematical optimisation techniques to derive parameters for a given constitutive model based on the stress-strain/load-displacement response measured in both laboratory and in-situ tests removing parameter selection subjectivity
9	<i>d</i>	Numerical modelling of creep in soft soils	Leoni, Vermeer	Numerical analysis of an embankment on soft soils using a new constitutive model for time-dependent behaviour of soft soils which accounts for anisotropy
10	<i>d</i>	Settlement analysis of foundation soil over a long time and comparison with field performance	Karim & Gnanendran	Modelling the consolidation of the foundation soil of a wide geogrid reinforced embankment using an elastic visco-plastic model
11	<i>b</i>	Effect of foundation embedment on consolidation response	Gourvenec & Randolph	Finite element study of the consolidation response of surface and variously embedded foundations in an isotropic elastic half-space considering the type of embedment and foundation-soil interface roughness
12	<i>a</i>	Digital specimen and digital test for granular materials	Fu, Wang Tümay, Kuang	Digital method to investigate the micro behaviour of granular materials and to generate 3D digital specimens
13	<i>a</i>	Experimental determination of statistical representative volume element in plane strain compression of dense sand	Jang, Chung, Kim & -H. Jung	Investigation on the representative volume element of a soil specimen in plane strain experiment, to appropriately account for wide variance of soil responses in computing average properties of granular soils using the digital image analysis technique
14	<i>a</i>	Three-dimensional desiccation modeling of very soft soils	Pak & Samimi	Developed finite difference code for modelling the desiccation phenomenon of very soft soils
15	<i>a</i>	Simulations of in situ water content and temperature changes due to ground-atmospheric interactions	Bicalho Cui	Numerical analyses to investigate the sensitivity of water content, pore-water pressure and temperature changes to the variations of the soil albedo value

3 MECHANICS OF SOIL, ROCK AND COMPOSITE MATERIALS

Several papers presented in Session 1b deal with the mechanical behaviour of soils, rocks and other construction materials

employed in geotechnical engineering, within a very large variety of practical applications.

Semi-empirical correlations mainly based on experimental observation, mathematical representation of soil time-dependent behaviour, complex non-linear constitutive models have been

presented, with extensive numerical support provided both by Finite Element and Discrete Elements methods.

Herein three topics among all are briefly recalled, i.e. the behaviour of cemented sand, unsaturated soil and asphalt mixtures, in which theoretical models have been successfully validated with experimental laboratory tests.

Some authors calibrated *stress-dilatancy* relationships which link mobilised friction with mobilised dilatancy, both for granular and fine coarse and cemented materials.

Zang & Salgado proposed a stress-dilatancy relation for cemented sands, alternative to Rowe relation. The Rowe stress-dilatancy relation both for uncemented and cohesive-frictional materials is based on the principle of energy minimisation. The Authors evidenced that this derivation is questionable, because the minimum energy principle is violated if friction is involved in the system, and even if the validity of the relation for uncemented sand has been proved, the validity for cemented sand has not been checked. Using Rowe's saw-tooth model together with the application of the laws of friction, the Authors derived in the transformed stress space (in which the material has the same ϕ' but no cohesion or tensile strength) a new form of the stress-dilatancy relation to use in Rowe framework.

A certain interest has been devoted to the behaviour of *unsaturated soils*, which characterised the shallow layers of natural deposit and the excavated, remoulded or compacted soils. Water is removed from the natural soil either by evaporation from the ground surface or by evapo-transpiration from vegetations. **Kawai et al.** referred of an accident in Poland where non-uniform settlement and building damage were caused by water uptake of vegetation. A constitutive model for unsaturated soil is needed for understanding the effects of degree of saturation and matrix suction on the mechanical behaviour.

Liu & Muraleetharan presented a comprehensive, coupled hydraulic-mechanical constitutive model, to simulate the behaviour of *unsaturated soils* in a general stress space, which accounts for water content variation, hysteresis of soil water characteristic curves, cyclic behaviour and anisotropic stress state. The hysteresis in soil water characteristic curves was modelled using concepts that parallel the elasto-plastic theory used to model stress-strain behaviour of soils. Matric suction was used as the stress variable and volumetric water content as the strain variable.

The constitutive model was calibrated and validated using complex triaxial tests on Toyoura sand under both monotonic and cyclic loadings. The model prediction are compared in Figure 2 with the experimental results.

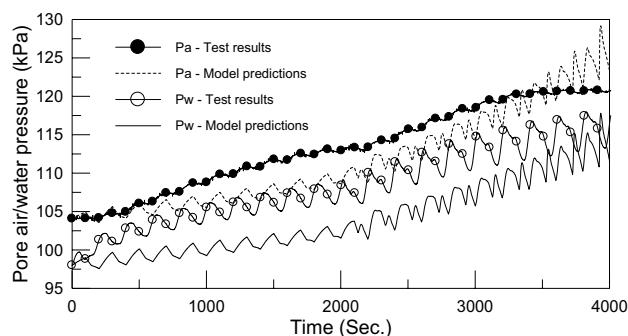


Figure 2. Measured and predicted pore air and pore water pressures, from **Liu & Muraleetharan**.

As far as the behaviour of composite material is concerned, **Soltani & Baziar** described results from creep and recovery tests and repeated uniaxial compression tests performed to identify and quantify the visco-elastic and visco-plastic components of *asphalt mixtures* response under creep and uniaxial repeated compression loading. The experimental results were used to identify the parameters of a visco-elasto-plastic

constitutive model, which predicts the mechanical behaviour of asphalt concrete material used in the construction of asphalt concrete core dam by decomposing the total strain into its visco-elastic and visco-plastic components and modelling the components separately. Figure 3 reports a comparison of the computed and the measured axial strains for constant strain rate condition. The Authors outlined the reliability of the visco-elasto-plastic model for predicting the material behaviour under one-way compression loading but, due to the difference between measured and predicted response, they evidenced that a corrective measure is needed to account for the effect of aggregate interlocking and damages.

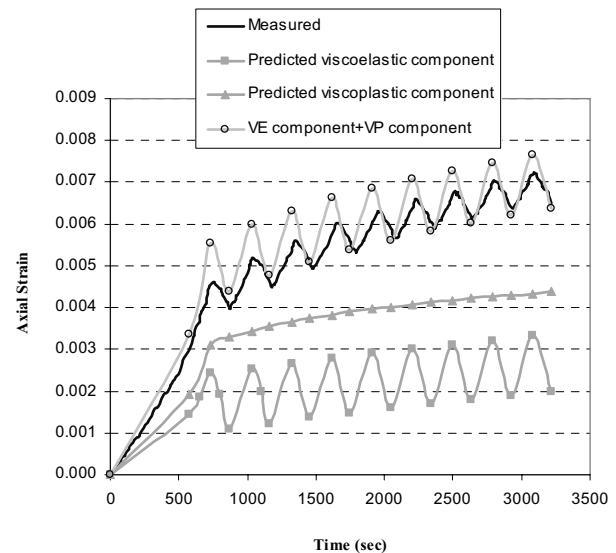


Figure 3. Axial strain history in constant strain rate test, from **Soltani & Baziar**

4 ONSHORE, OFFSHORE AND "EXTRATERRESTRIAL" SHALLOW AND DEEP FOUNDATIONS

The papers presented in this Session treated various application topics varying from bearing capacity under vertical and combined loads even in low gravity conditions, to prediction of consolidation settlements, stress induced by the foundation and distribution within the soil mass, behaviour of mixed foundations.

Shallow foundations

The evaluation of the stress increment induced in the soil by a shallow foundation is generally performed using the elasticity theory.

Ejjaouani et al. presented 3D stress calculation model in which the dimensions of the influence zone of a surface load are defined by a stress diffusion angle β . Within a certain depth z_{pl} from the foundation bottom the angle β is assumed dependent on the nature of the soil and on some of the geotechnical characteristics, such as density and void ratio. Below z_{pl} β is considered equal the angle of shearing resistance. In the proposed calculation model the variations of the vertical stress increments on each horizontal plane of the soil mass are described by a third order polynomial equation.

As far as the shallow foundation bearing capacity is concerned, in their paper **Hossain & Randolph** summarised traditional design approaches and recently published solutions for evaluating ultimate *vertical capacity* of onshore and offshore shallow foundations on single and double layer clays.

They found that for pre-embedded foundations, traditional approaches provide good estimates of bearing capacity for surface footings on relatively uniform clay, while adjustments are required for embedded foundations, particularly in the case of clay with increasing strength profile and layered clay

profiles, where the upper layer has significantly higher strength than the lower layer. For offshore spudcan foundations, recommended design approaches are currently based on inappropriate models of the soil deformation patterns, leading to significant underestimate of the bearing capacity for single layer clays. On stiff-over-soft clays, traditional approaches give poor estimates of the potential for punch-through failure and its degree of severity.

Therefore the Authors provided improved design approaches for circular pre-embedded foundations on single layer and stiff-over-soft clays and for spudcan foundations, including approximate allowance for the effects of softening (Figure 4).

When a shallow foundation is subject to *combined loading*, the bearing capacity characteristics can be expressed as a bearing capacity locus in the generalized load space (V, H, M/B), where V, H and M are vertical, horizontal and moment loads acting on a shallow footing with the width B, respectively. It is widely accepted that a shape of a bearing capacity locus is a cigar-like shape.

Kobayashi & Izawa presented a hybrid type rigid plastic FE method to evaluate the bearing capacity of shallow footings subject to combined loading conditions, which implements the interactions along the interface of a footing and a soil, such as contact/separation and slippage, modelled as simple rigid plastic inequality constraint conditions. Bending failure of strip foundation structures is also modelled as rigid plastic inequality constraint conditions. The proposed method has been applied to a strip footing to investigate the bearing capacity characteristics.

The numerical results have been summarised as a bearing capacity locus in a generalized load domain V, H, M/B. The Authors found that for weightless $c, \phi = 0$ soils, horizontal bearing capacity mainly depends on the friction along the interface of the soils and footings, as shown in Figure 5. Combination of horizontal and moment loads is also important and positive - positive combination shows larger capacities. However, these differences decrease with the decrease of friction along the interface.

For c, ϕ soils, as the effect of self weight increases the failure mechanism enlarges mobilising larger bearing capacity.

As to the bearing capacity under vertical loading of *extraterrestrial foundation*, the future lunar exploration will certainly request in the next years the development of new design approach to ensure the success of lunar operations such as excavations, mining and foundation works for extraterrestrial facilities, operations which need a deep understanding of the soil-machine and/or soil-structure interaction problems in a low gravity environment.

In this framework, **Kobayashi et al.** presented the results of a series of model tests of shallow footing systems on a simulated lunar soil and Toyoura sand conducted in partial gravity fields, aimed at studying the effects of gravity on load-settlement characteristics of shallow foundation systems, and at theoretically evaluating the dependence of the ultimate bearing capacity on gravity. The loading tests were performed on an aircraft that flew in parabolic paths to generate partial gravity fields.

Figures 6 and 7 show that the gravity hardly influences the coefficient of subgrade reaction K_s for the lunar soil simulant, whereas k_s is proportional to the gravity level for Toyoura sand. The ultimate load q_u values of Toyoura sand are in proportion to the gravity levels, regardless of how it is packed, whereas no clear proportionality between the gravity levels and the q_u values can be found in the case of the lunar soil simulant.

The adopted Particle Image Velocimetry technique evidenced a general shear failure mode in Toyoura sand and the formation of a compression region below the footing in lunar soil simulant. The Authors explained that in the general shear failure mode as seen in case of Toyoura sand, the passive failure zone spreads upward until the failure surface extends through the ground surface, causing the surface to swell. At that

moment, the zone moving upward is doing work against gravity, and this appears to be the major factor in determining the dependence of the ultimate bearing capacity on gravity. In the case of the local shear failure mode downward displacements are predominant and, thus, there is no work against gravity.

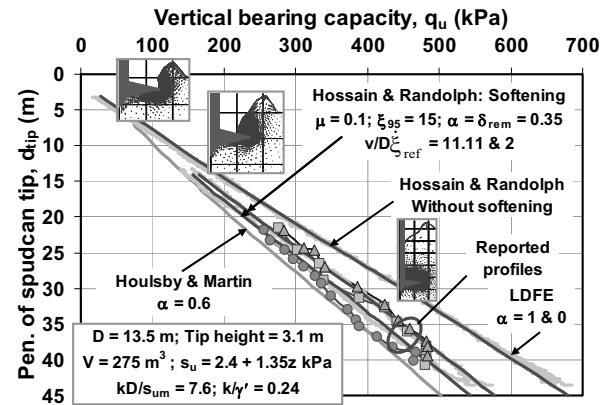
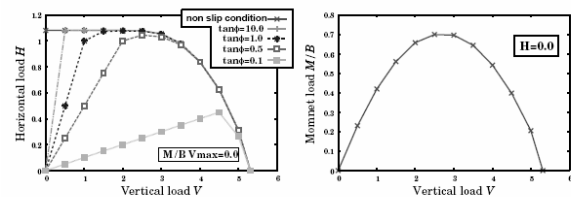
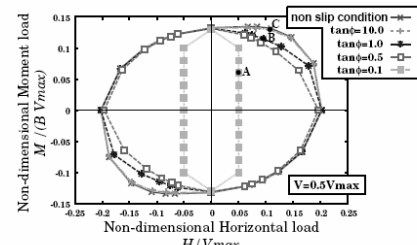


Figure 4. Comparison among LDFE results, Hossain & Randolph approach, SNAME approach and reported field data (single layer clay). [Rate effect: μ is relative strength change per decade of strain rate change; softening: ξ_{95} is cumulative plastic shear strain for 95% remoulding, δ_{rem} is inverse of soil sensitivity], from **Hossain & Randolph**.



(a) On $M/B = 0$ plane (b) On $H = 0$ plane



(c) On $V/V_{max} = 0.5$ plane

Figure 5. Cross-sectional views of bearing capacity loci (weightless $c, \phi = 0$ soil), from **Kobayashi & Izawa**.

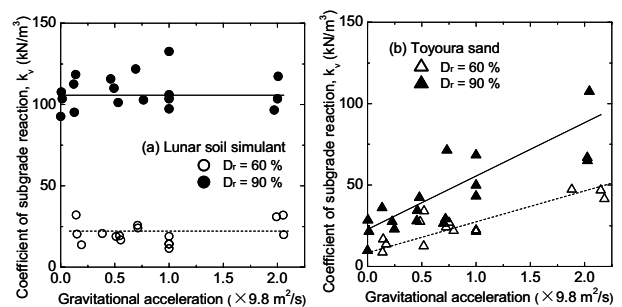


Figure 6. Effects of gravity on on subgrade reaction, from **Kobayashi et al.**

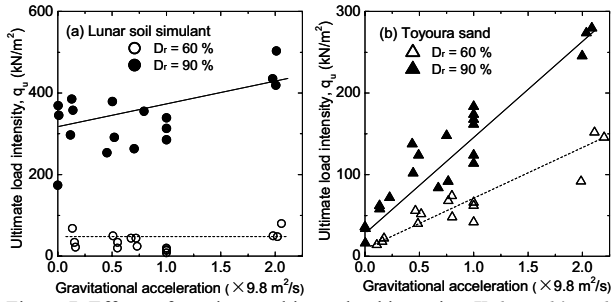


Figure 7. Effects of gravity on ultimate load intensity, Kobayashi et al.

If cycling loading are also concerned, as for of machine foundations, the design can be based on several methods such as the dynamic impedance function, which has been calculated for various conditions by analytical, semi- analytical and numerical approaches.

Jafarzadeh et al. presented the results of small scale physical tests performed to provide experimental data necessary for the verification the dynamic impedance function, with particular attention to the effects of the inertia, of the dynamic load level and of the footing embedment on the dynamic response of foundations. From the experimental results, the Authors concluded that inertia of footing has effect in moderate and high frequencies in dynamic response of foundation and it can affect both the stiffness and the damping coefficient. Damping of system is relatively constant for various dynamic loading levels while dynamic stiffness is constant under a certain frequency value, above which it decreases by increasing intensity of loading. The test results showed also a decrease of dynamic stiffness due to increasing depth of embedment, while the dashpot coefficient is relatively constant.

As to the settlements induced by shallow foundations, Gourvenec & Randolph presented an investigation into the consolidation response of surface and variously embedded foundations in an isotropic elastic half-space.

A buried plate, a solid structural foundation and a skirted foundation were modelled, with both smooth and rough surfaces. The soil was represented by a homogeneous elastic half-space with Biot-type consolidation governing the stress-pore fluid coupling and constant and isotropic elastic parameters and permeability were assumed in all analyses.

The results showed that embedment generally reduces the magnitude and rate of consolidation settlement due to the resistance of material above foundation level and the increased drainage path length; the magnitude and rate of consolidation settlement reduces still further for rough-sided foundations due to the portion of foundation load carried by side friction (Figure 8). The reverse trend is observed for smooth skirted foundations due to one-dimensional compression within the soil plug. The authors outlined that the effects of heterogeneous stiffness, plasticity and yielding, as well as permeability dependence on void ratio, anisotropic permeability and a range of embedment ratios would provide better understanding of the consolidation response of embedded foundations.

Deep foundations

The bearing capacity of an existing shallow foundation can be significantly improved by the introduction of sheet piles around the periphery. In the resulting skirted footing the primary load from the superstructure is transferred to the subsoil by the shallow foundation and the sheet pile system is mainly an auxiliary system to reduce settlement and tilting and to increase the pull out capacity.

Punrattanasin et al. presented 1g physical model tests executed to investigate the effect of sheet pile length to the capacity of existing shallow footing in sand subject to vertical loads. Test results demonstrated that sheet piles increase the vertical capacity of shallow footing and the longer sheet pile length provides the higher vertical capacity. The improved

capacity can be attributed to the end bearing of square footing, to the transfer of load to deeper soil through the skin friction of sheet piles and to the confinement effect of soil inside the footing. Figures 9 show the response of ground after testing a shallow and a sheet pile foundation. The mode of failure for the two types of foundations can be identified as general shear failure. The soil below the shallow foundation is moved to the lateral sides and the failure surface in the soil extends to the ground surface. For the case of sheet pile foundation, the soils is also moved to the lateral sides but the size of failure surface outcrop is smaller than that of the case of shallow foundation. The comparison between construction cost and the foundation capacity can provide an appropriate sheet pile length.

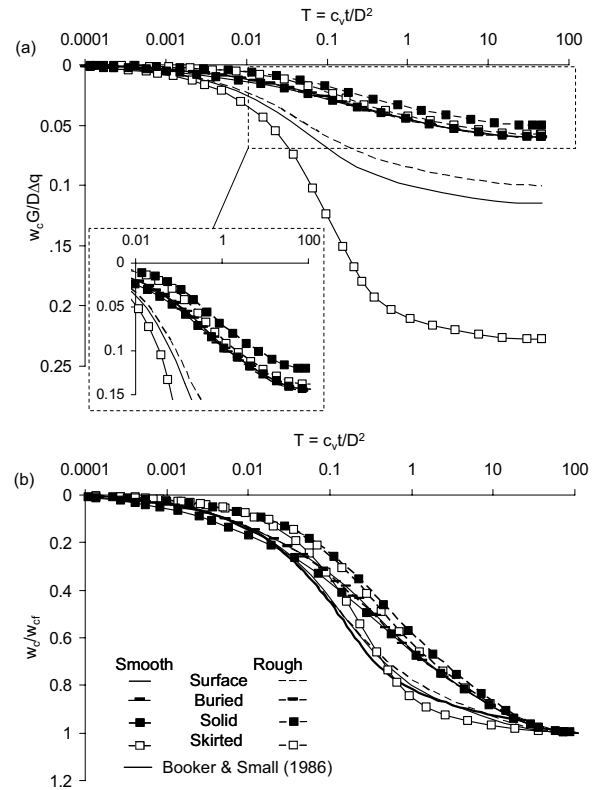


Figure 8. Settlement time histories, from Gourvenec & Randolph.

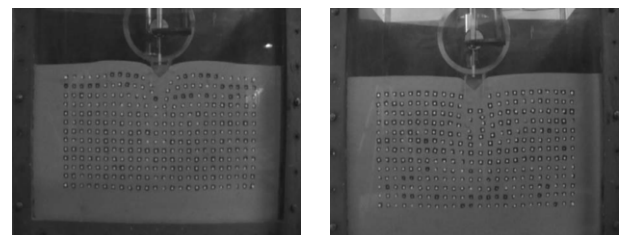


Figure 9. Ground response after loading tests on shallow (left hand-side) and sheet pile (right hand side) foundations, from Punrattanasin et al.

Türkmen & Ergun performed laboratory load tests on models of piled raft in kaolinite clay to study bearing and sharing behaviour of composite foundations. The isolated pile, the unpiled raft and the piled rafts with 2, 4, 7, 9 piles were tested. The Authors observed that at the initial loading stages nearly the entire applied load is carried by the piles; as the settlements increase the full capacity of piles is mobilised and the raft starts to share more load. The initial load sharing proportion depends on the number and capacity of piles.

The load bearing capacity of a pile which is part of a piled raft is improved respect the isolated pile due to the raft contact pressure with the ground which enlarges the pile shaft capacity.

On the other hand the Authors observed that the increasing number of piles reduces the load carried by each pile.

This could be the effect of the interaction between the displacement fields produced by the settlement of each pile, which causes a tangent stiffness decrease. Figures 10 and 11 show the results of centrifuge tests on models of circular rigid piled raft (Fioravante et al. 2008a). Figure 10 shows that while the load-bearing behaviour of a single isolated pile can be described as ductile, the results obtained for the pile beneath the raft suggests an enhanced pile response due to the increment of vertical and horizontal stresses provided by the raft pressure at the soil surface (hardening behaviour). In Figure 11 it can be seen that the ultimate total load augments when the spacing reduces but the stiffness at small settlement progressively decayed.

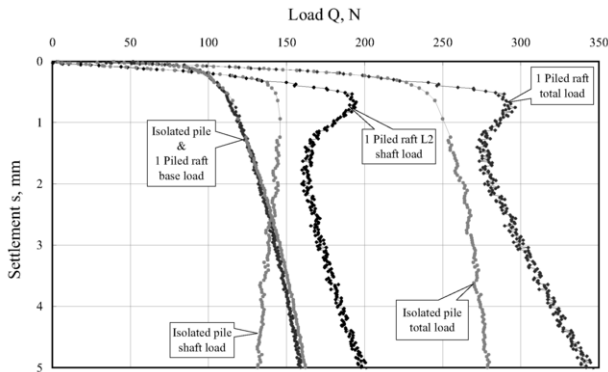


Figure 10. Load settlement behaviour of an isolated pile and a single pile beneath a circular rigid raft, model scale (Fioravante et al. 2008a).

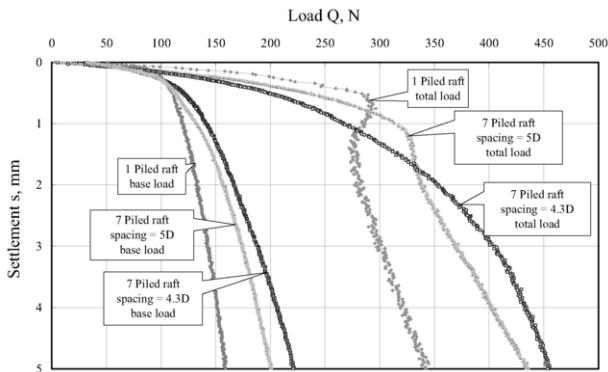


Figure 11. Total and base capacity of the central piles of the 7 piled rafts, model scale (Fioravante et al. 2008a).

With reference to the MOSE mobile barriers, projected to safeguard Venice lagoon from high tides and described by Jamiolkowski et al., to compare the load transfer mechanisms and the load sharing between a rigid raft and a group of piles in direct contact with the raft or separated from the raft with and interposed granular fill layer, a series of centrifuge physical model tests (Fioravante et al. 2009) and a series of numerical simulations using the TOCHNOG code (Bonizzoni and Daprat 2006) have been performed.

The MOSE mobile barrier system consists of a series of caissons installed at the bottom of three lagoon inlets; the caissons lie on piles driven after dredging the inlet bottom and then covered by a 1 m thick layer of compacted coarse grained granular material. The piles were aimed at mitigating the differential settlement due to the spatial soil variability and to any possible placement imperfection linked to the complexity of underwater works (i.e. settlement reducing piles). The granular fill has been designed to reduce constraint reactions between the piles and the caissons during cyclic excitation and to realise a uniform pressure distribution which prevents local failures of the contact piles (Jamiolkowski et al.).

Both physical and numerical modelling show that the placement of a granular layer between the caisson bottom and the piles heads generates a negative shaft friction over almost the upper half length of the piles, see Figures 12 and 13. The

phenomenon can be attributed to the circumstance that the insertion of a deformable layer between the caisson's slab and the piles head inhibits the effective displacement compatibility between the raft and the piles. Such a mechanism is mainly governed by the thickness and the stiffness of the interposed layer.

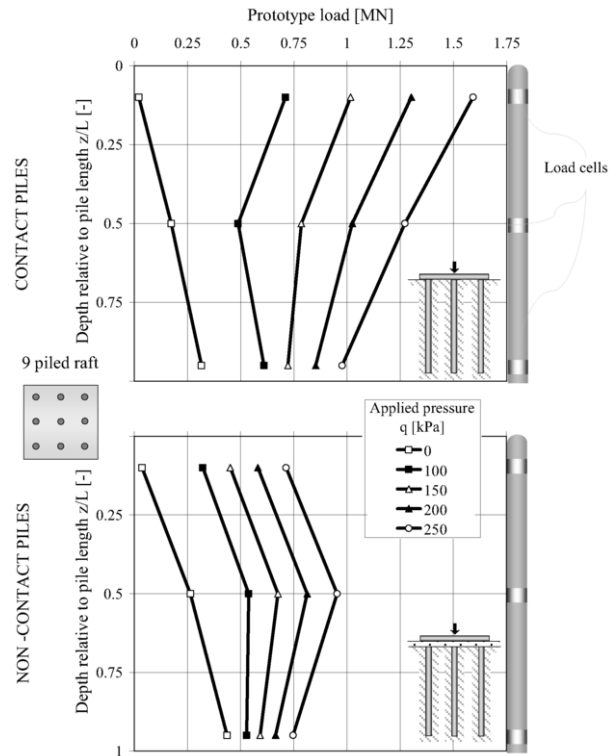


Figure 12. Average axial load distribution with depth from centrifuge tests (Fioravante et al. 2009).

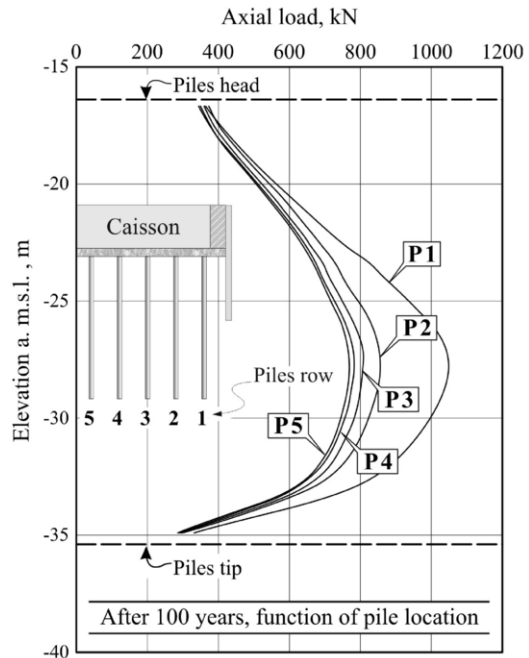


Figure 13. Load distribution along piles from centrifuge tests, from Bonizzoni and Daprat 2006.

New modelling techniques for shallow and deep foundations

An new interesting testing material has been employed by some researchers: *transparent soils*, made of either transparent

amorphous silica gels or powders with a pore fluid having the same refractive index. Conventional geotechnical tests showed that transparent soil exhibited macro-geotechnical properties similar to those of natural soils. A comparison study also showed that transparent soils can be used to simulate natural soil in model tests.

Transparent soil was used by **Song & Hu**, for centrifuge tests performed to study in-lined pullout of suction embedded plate anchors. After installation, a mooring line attached to the plate anchor was tensioned, causing the plate anchor to rotate to an orientation perpendicular or almost perpendicular to the pullout direction. The loss in anchor embedment during keying, which represents a non-recoverable loss in potential anchor capacity, was quantified by inspecting anchor movement in the transparent soil models and it was correlated to the chain displacement measured during keying. Figure 14 reports four digital images from a transparent soil test.

The experimental data were compared with large deformation FE analyses, and both centrifuge and FE results showed that, during inclined anchor pullout, the anchor experiences chain cutting soil, initial rotation to half-way, full rotation and anchor capacity development.

The Authors observed that the good agreement between the experimental and numerical results suggests that the numerical approach is robust to provide design information when anchor is simulated appropriately and it can be used as a practical tool when anchor geometry varies. They proposed a correlation between the loss in anchor embedment and the chain displacement.

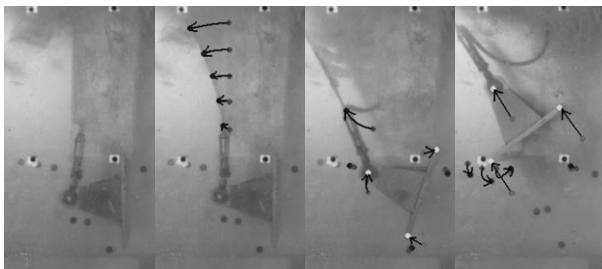


Figure 14. Transparent soil test, from **Song & Hu**.

Liu & Iskander presented non-intrusive measurement of deformation inside a transparent soil model to visualise the 3-D internal deformation and strain field under a model footing. In the research silica gel was employed for modelling sand and silica powder for clay. The laser speckle photography technique was used to obtain the displacement field by cross-correlating two consecutive images captured before and after the deformation.

The tests set-up consisted of a CCD camera, a laser light source, a loading frame, a precision stage, and a PC for image processing. A model footing with a plan dimension of 50x25 mm was used to simulate a continuous footing with a width of 25 mm. The results show that transparent soil and developed optical system are suitable for studying 3-D deformation measurement in geotechnical engineering.

The paper from **Gaudin & White** proposed newly-developed centrifuge modelling techniques for simulating the dynamic laying of seabed pipelines. The two examples presented highlighted the complexity of the pipeline motion at the touchdown zone and the effect on the as-laid pipe embedment, and evidenced the effectiveness of physical modelling to replicate complex geotechnical problems providing an immediate representation of the design situation.

Due to the curved surface of a pipe, the soil surrounding the pipe must deform and fail as the pipe is laid on the seabed and this remoulding is enhanced by vertical and horizontal cyclic motion at the touchdown point of the pipe due to heave of the lay vessel. This complex loading process makes the remoulding of the soil difficult to assess or to model. The performed

centrifuge tests provided quantification of the as-laid embedment of a pipeline; the Authors evidenced that physical modelling not only can be directly used for design, but can provide important benchmarks for reliable analytical models.

5 SLOPE STABILITY, EARTH PRESSURE AND RETAINING STRUCTURES

A number of examples of *physical model* tests to study the static and dynamic behaviour of debris flows, slope and retaining structures, retaining walls and reinforcing elements have been presented.

As to *debris flows*, which pose a major hazard in regions where mountainous terrain and high runoff co-exist, **Bowman & Sanvitale** presented results of an experimental research using a flume apparatus to evaluate the role of particle size distribution on the mobility of flowing granular materials at a given moisture content (velocity and run-out length) and showed that a well-graded material travel far and fast before final deposition (Figure 15). The experiments outlined that as C_U increases so does the run-out length and the velocity and the relationship between the square of the velocity and the run-out is non-linear as shown in Figure 16.

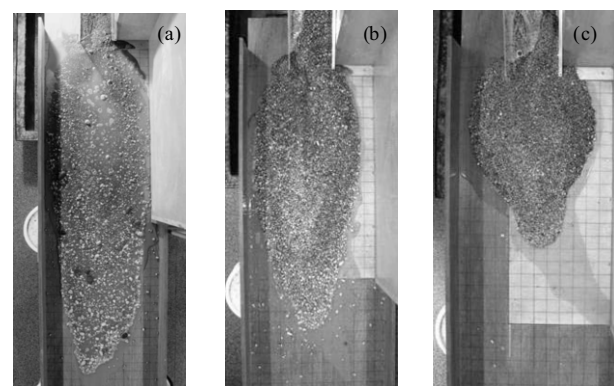


Figure 15. Test depositions for particle size distributions with same D_{50} but different C_U : (a) $C_U = 21$, (b) $C_U = 6.4$, (c) $C_U = 3.3$, from **Bowman & Sanvitale**.

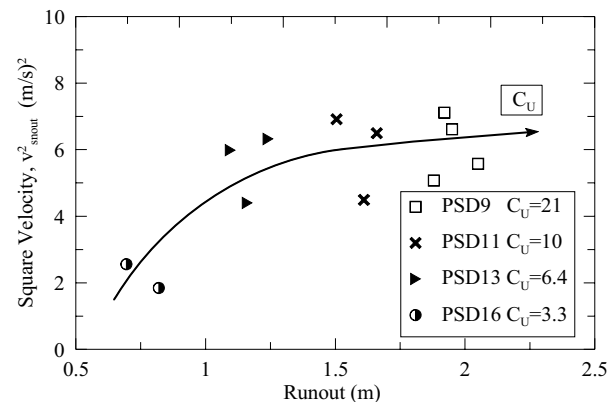


Figure 16. Square value of front velocity against run-out for tests with same $D_{50}=1.76$ mm, from **Bowman & Sanvitale**.

The slopes are at greater risk of failure during *slope cutting works*, and slope failures have often occurred suddenly without any clear signs of failure, as evidenced by **Itoh et al.**, performing full-scale and centrifuge model tests on slopes; they examined the failure mechanisms due to progressive cutting works and observed that local slope failures occurred before a complete failure.

As shown in Figure 17, an excavated height of 2.5 m (full scale slope) caused about 4 mm of slope displacement and slope deformation continued to increase till a local failure was

observed. Finally, a large-scale collapse from the slope crest occurred immediately after the excavated height reached 3 m.

From the experimental observations the Authors argue the possibility of predicting slope movement during excavation before failure by measuring vertical and horizontal displacements of benchmarks placed at the slope crest.

The experience presented is remarkable since it compares centrifuge to full scale tests performed under equivalent conditions (Figure 18); it evidences the capability of centrifuge modelling to well reproduce the mechanisms of a boundary value problem (conditions and shape of slope failure).

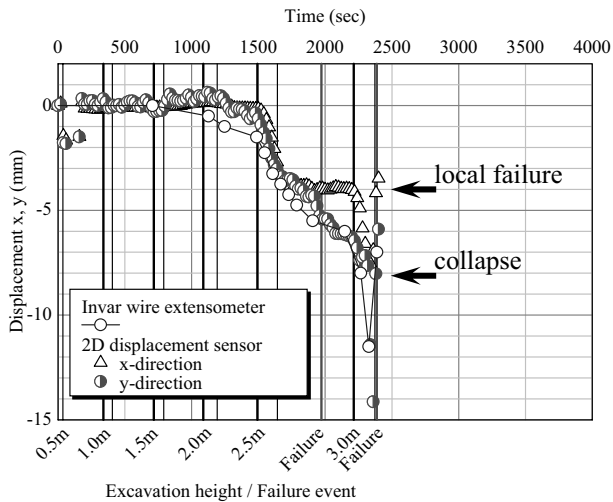


Figure 17. Slope movements in the field test F2, from *Itoh et al.*

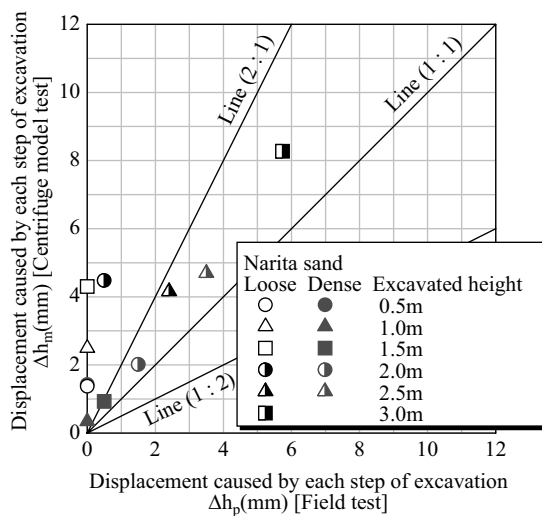


Figure 18. Direct comparison of the measured displacement caused by each step of slope cutting in the field test and centrifuge model test, from *Itoh et al.*

Design procedures of retaining structure should take into account for seismic active earth pressure, since seismic earth pressure under large earthquake loads has not been extensively evaluated in the literature. *Watanabe & Tateyama* presented a series of shaking table tests performed on retaining wall models and compared the seismic earth pressure measured on the backface of retaining wall with the Mononobe-Okabe theory.

Gravity type retaining wall model was used and both normal and shear components of seismic earth pressure were monitored. The subsoil model was made by well-compacted gravel and an iron plate, covered with sand paper, was fixed on the subsoil so that the major failure mode was lateral sliding; two different friction angles between retaining wall model and iron plate, were employed. The models were subjected to large irregular excitation.

The Authors observed that seismic active earth pressure acting on the retaining wall was largely smaller than that obtained by Mononobe-Okabe theory. Even though the earthquake load was large, only a small seismic earth pressure acted on the low stability retaining wall. This was because the retaining wall moved outward by the inertia force more than the backfill (Figure 19). The maximum seismic earth pressure and the location of failure plane under large seismic load were produced by a “critical” acceleration, lower than the maximum value experienced.

The Authors proposed to use the critical acceleration instead of its maximum value within the Mononobe-Okabe theory to evaluate the maximum seismic earth pressure and the location of failure plane. This gives a reasonable earth pressure under large seismic load, which agrees with the experimental values.

The Authors outlined the necessity to establish a rational method to evaluate the residual displacement of the retaining wall. This is one of the remaining issues for establishing the seismic design procedure of retaining walls.

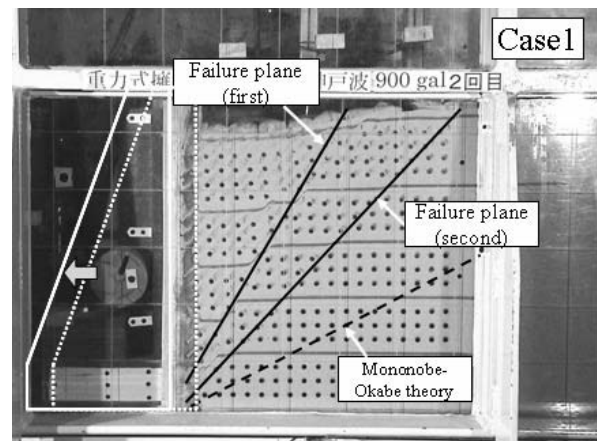


Figure 19. Residual displacement of wall and formation of failure plane (at the end of second shaking test) from *Watanabe & Tateyama*.

Izawa & Kuwano presented results of tilting table and shaking table centrifuge tests on geogrid reinforced soil walls (GRSWs), focusing on the effect of the tensile stiffness of geogrid and the properties of backfill soils on seismic performance of reinforced walls.

In the centrifuge tilting table tests, pseudo static horizontal loading was applied by tilting the models. In the shaking table tests, sinusoidal seismic waves were applied to the model with gradually increasing amplitude of acceleration.

The model of GRSWs subjected to pseudo static loading failed due to sliding when the inclination of the wall at bottom reached a critical value, independent on tensile stiffness of geogrid, and slip line generated. The Authors considered that such slip line generated when the backfill itself in reinforced area reached to failure. In the centrifuge shaking table tests, the models showed almost the same deformation modes. The model GRSWs did not collapse even after the slip lines occurred in the centrifuge shaking table tests. However, after formation of slip line, sliding displacement along the slip line became significant.

As in Reinforced Earth walls, *Ribbed anchors* are widely used in geotechnical engineering applications.

An experimental study into the pullout resistance of ribbed anchors in sands was carried out in a triaxial testing tank by *Irsyam et al.* The experiments were carried out on both dense and loose sands at various confining pressures adopting five types of anchors.

The authors evidenced that ribbed anchors can significantly increase the pullout resistance and enhance the transfer of stress between soil and the inclusions. The transfer of stress occurs by two basic mechanisms; friction and passive soil resistance with both mechanisms acting simultaneously.

The values of coefficient of apparent friction at peak, μ^*_{peak} and residual, μ^*_{res} for smooth, rough, and ribbed anchors and for dense condition are shown in Figure 20, where $\mu^* = \tau_n / \sigma_n$ and τ_n and σ_n are the shear stress (including passive resistance from rib) and the applied normal stress.

For ribbed anchors, the contribution of passive resistance against the ribs resulted in a higher coefficient of apparent friction (μ^*) for both the peak (μ^*_{peak}) and residual loading conditions (μ^*_{res}) compared to that of smooth anchors.

The rib spacing resulted an important factor controlling peak and residual anchor resistance and the μ^* for both dense and loose sand. An increase in rib spacing enlarged the peak strength and μ^* , up to an optimum rib spacing of 12 mm. Beyond the optimum spacing, however, an increase in rib spacing decreased the shear resistance.

As the authors pointed out, the rib spacing has an important role in controlling a zone of dilation for dense sand and a zone of contraction for loose sand. They observed that for rib spacing smaller than optimum, part of the grains between adjacent ribs were trapped and moved as a unit with the anchor, giving a smaller anchor resistance. For rib spacing beyond optimum, part of the anchor surface between adjacent ribs acted as a smooth anchor where grain slipped.

The results present by the Authors contribute to the studies currently undertaken by many researchers since the load transfer mechanisms between the soil and rigid inclusions is of great interest for the understanding of many applications, from the behaviour of soil reinforcing to the shaft resistance mobilisation of deep foundations which are governed by the behaviour of the interface zone.

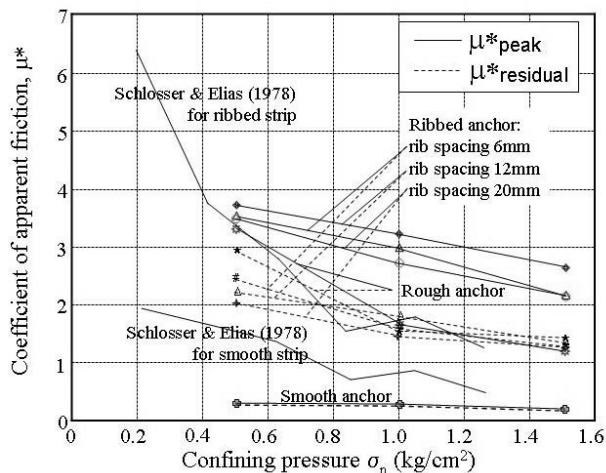


Figure 20. Apparent coefficient of friction versus confining pressure for dense condition from *Irsyam et al.*

The interface zone is subjected to large plastic straining, as result of load imposed on the inclusion. The tendency of the interface to change its volume interacts with the behaviour of the surrounding soil and the stress normal to the interface can increase or decrease when soil exhibits dilative or contractive behaviour respectively (Wernick, 1978, Boulon & Foray, 1986, Boulon, 1988, '89). It results in an actual value of the σ_n which differs from the applied one and which should be taken into account in the evaluation of μ^* .

Moreover, if shear failure occurs in the soil surrounding the inclusion, the soil body enclosed within the shear bands should be taken into account in the computation of the shear resistance (i.e. the diameter of the inclusion should be enlarged of an amount depending on the interface zone thickness).

6 EMBANKMENT AND GROUND IMPROVEMENT

Many of the presented papers dealt with embankment. Two interesting papers were concerned with the effects of seepage

and/or flood conditions on the stability of embankments in case of river dikes or dams.

The conditions within dams and dykes, where the seepage water can cause *subsurface erosion failure* when the water flow reaches a critical value, have been studied by *Boley & Lenz* by means of physical model tests. The models reproduced the water flow within a coarse filter material placed between a fine grained layer, which reproduced the sealing base layer of a dyke, and a clay bed which modelled the natural subsoil. Above the base layer a pressure device reproduced the weight of the embankment. The main focus of the investigations was the verification of the influence of the stress and the filter grain size on the critical hydraulic gradient. The tests showed that higher vertical stress and/or finer filter material produces higher critical hydraulic gradient, while finer base material produces lower critical hydraulic gradient.

Measured critical hydraulic gradients were compared with the values obtained using a mathematical model, which, defining a transition zone where the filter material doesn't exist neither in solid state nor in fluidity, evaluates the critical velocity as a combination of solid and fluid critical velocities. To determine the critical hydraulic gradient, the critical velocity has to be integrated in a non linear flow law. Figure 21 shows the test results compared to that of the theoretical model, which, as the Authors evidenced, seems to provide a conservative estimation of the critical hydraulic gradient.

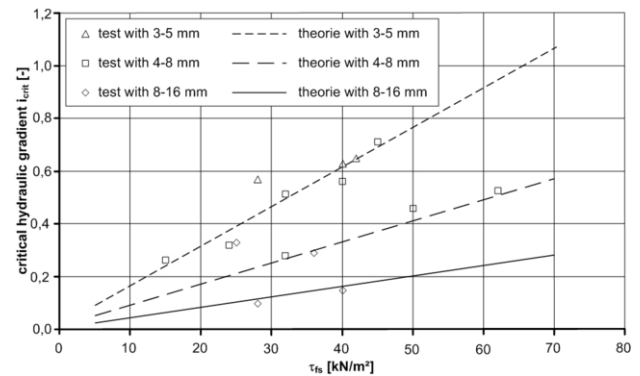


Figure 21. Theory and test results for the flow parallel to the layer, from *Boley & Lenz*.

Matsumaru et al. presented the results of shaking table tests on model embankment affected by seepage water, with intention of evaluating the *effect of seepage* on seismic resistance and of developing a method of calculation of the residual displacement during earthquake. From the shaking table test the Authors observed that the embankment deformed as the shape of the circular slips, which were activated when the amplitude of the input motion reached its maximum value and the maximum amplification was measured at the top of the embankment. The embankment started to deform plastically from this time, the response of the embankment changed from the amplification to the damping and the pore water pressure started to increase rapidly.

Based on these results and accordingly with the Japanese design standard for railways, the Authors proposed for the evaluation of residual displacement during earthquake to use the Newark method taking account for the influence of the water level and the degree of saturation on the values of the cohesion and the angle of shearing resistance. The validity of this method was checked by simulating the shaking table tests, referring to the water level and degree of saturation determined by the experimental results. The calculated displacements resulted almost coincident with the measured values.

As far as embankments on soft ground are concern, consolidation and creep settlements can be predicted form in situ, laboratory and numerical analyses, as reported by *Jamiołkowski et al.* and *Karim & Gnanendran*.

The settlements of the MOSE mobile barriers were predicted on the base of extensive geotechnical investigation and a large scale and heavily instrumented trial embankment. The trial embankment was decided by the contractor Consorzio Venezia Nuova due to the intrinsic difficulties related to the spatial heterogeneity of the lagoon deposits and of the predominant presence of difficult to sample soils.

Figure 22 reports the construction history with the settlements measured under the trial embankment centre where the stress and the deformation condition replicate that of the 1-D compression. During the embankment construction, occurred a nearly entire consolidation settlement.

The secondary compression coefficient, as referred to the defined vertical strain ($C_{\alpha\epsilon}$), has been evaluated from the field settlement curves inferred from the sliding deformer readings and from laboratory oedometer tests. The comparison $C_{\alpha\epsilon}$ (field) against $C_{\alpha\epsilon}$ (lab), see Figure 23, suggests that in fine grained soils the field values are, on average, 50% higher, while in coarse grained materials their ratio is near the unity.

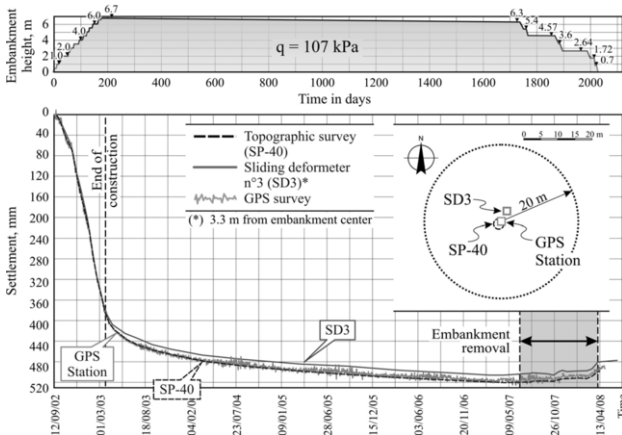


Figure 22. Time-settlement curves at the centre of the trial embankment, measured with different types of instruments, from *Jamiolkowski et al.*

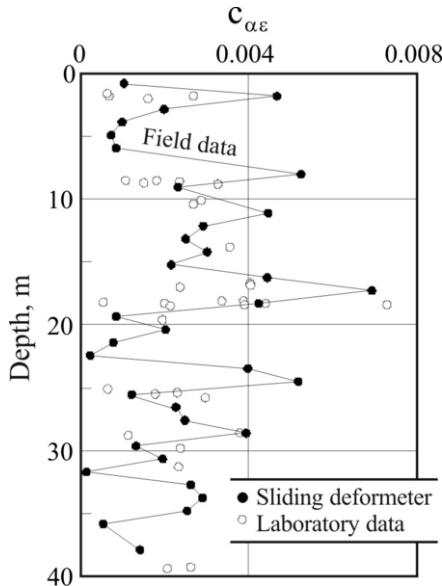


Figure 23. Comparison between field and laboratory secondary compression, from *Jamiolkowski et al.*

On the other hand, to model the long term settlement and pore water pressure response of the soil near the centre-line of a wide geogrid reinforced embankment a non-linear creep function has been used by *Karim & Gnanendran* in association with an elastic visco-plastic model for time dependent behaviour. The embankment, 300 m long and 60 m wide at ground level, was constructed over a swamp located 150 km

north of Sidney, on very soft alluvial clay of about 16 m thickness, whose mechanical properties were improved using surcharging and prefabricated vertical drains, and the construction was staged using light-weight fill materials and wide stabilising berms.

The performed simulation well reproduced the final settlement of the embankment near the centre line with higher accuracy with respect a modified Cam clay with a constant creep coefficient, as reported in Figure 24.

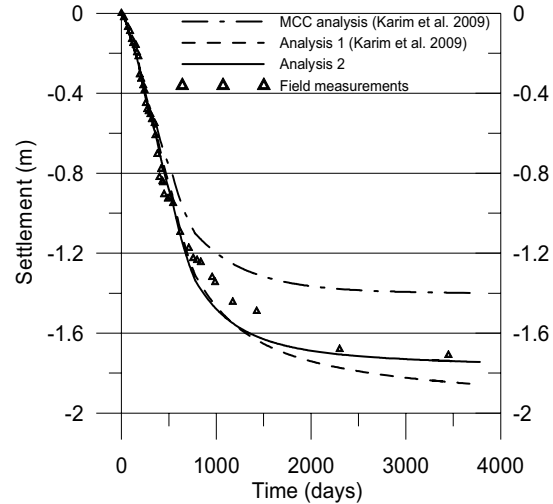


Figure 24. Time vs. settlement from three different analyses, from *Karim & Gnanendran.*

A countermeasure to prevent excessive consolidation and creep settlements of embankments on soft ground consists on reinforcing the subsoil with rigid inclusions (piled embankment).

The driving of a rigid inclusion in soft soils can be viewed as a radial undrained cavity expansion process, which produces densification and consolidation of soft soils in the radial direction. *Biringen et al.* presented the results of physical model experiment aimed at quantifying the stiffness and strength improvement obtained by the lateral preloading exerted by a driven pile. In the model test, initial anisotropic normal consolidation of a kaolinite clay model was achieved by increasing the vertical load under K_0 -conditions, then a pile was rapidly inserted in the soil model under essentially undrained conditions, allowing dissipation of excess pore water pressure through the top and bottom-plate drainage; finally multiple vertical load applications on the soil surrounding the model pile were performed at zero lateral strain. Bender elements were employed to monitor changes in the stiffness of the soil surrounding the pile at various radial distances and Vs tomographic images were created. The images indicated an increase in Vs and thus in soil stiffness around the driven pile. Results were further supported by vane shear strength and moisture content measurements, indicating an increase of in undrained shear strength and a reduction of 7% in water content.

The seismic behaviour of an embankment lying over a pile-reinforced soil has been studied by *Thai Son et al.*, the stability analysis was based on the implementation of a multiphase model extended to elasto-plasticity.

The multiphase modelling, consisting in a substitution of the reinforced zone with a superposition of a continuum made of two interactive phases (matrix and reinforcement), was compared with a 3-D numerical simulations with elasto-plastic model implemented, in which the rigid inclusion were individually simulated. The preliminary results showed the rising of the displacement of a characteristic point of the embankment as the horizontal acceleration increases and the comparison with the numerical simulation was encouraging.

7 TUNNELLING

The main issues when dealing with shallow tunnelling are the relationship between the *volume loss* and the *surface settlement* and the interaction effect between tunnelling and existing structures. In the Session 1b the impact of tunnelling on piled structures have been studied by *Shahin et al.*, which presented results of 1g model tests and numerical simulations (carried out with the same scale and the same boundary conditions of model tests and performed using the “subloading t_{ij} model”) on tunnel excavation. They considered two types of excavation patterns: fixed centre and fixed invert excavation, with the same amount of shrinkage applied.

As the physical and numerical results have shown, surface settlements, earth pressure around tunnel and ground movement are significantly influenced by the displacement applied at the tunnel crown for the same overburden and the same volume loss: the surface settlement is larger in the case where the invert is fixed than that of the fixed centre excavation, the difference of the surface settlement profiles being greater for shallow tunnelling.

Therefore the Authors concluded that for shallow tunnelling the surface settlement may not be properly estimated using the method of volume loss. Figure 25 shows the distribution of shear strain for fixed centre and fixed invert excavation, in free-field conditions, for one of the analysed model. The shear bands developed from the tunnel invert and covered the entire section for the fixed centre excavation, while developed from the side of the tunnel for the fixed invert excavation. The range of the deformed region for the fixed invert resulted narrower compare to the fixed centre excavation.

The existing building load influenced very much on the subsidence of the building, as well as on the surface settlement and earth pressure due to tunnelling. The physical and numerical analyses evidenced that the distance between the pile tip and the tunnel crown plays an important role on the piled raft behaviour.

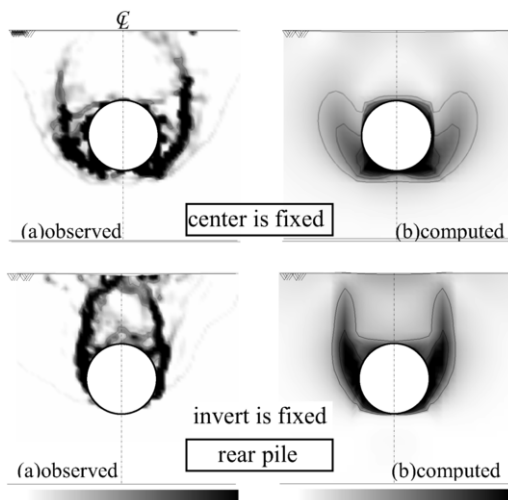


Figure 25. Distribution of shear strain: freefield, from *Shahin et al.*

The effects of soil long-term behaviour for existing tunnel in material whose mechanical behaviour is time-dependent have been presented by *Sekine et al.* The purpose of their study is to propose an effective evaluating method for the long-term stability of existed tunnel in soft rock. By comparing the results of model tests (two types of tunnel model tests, failure and constant load creep test, were executed on a manmade soft rock) with the corresponding 2D finite element analysis (based on an elasto-viscoplastic model) the effectiveness of the proposed numerical method has been verified.

The simulated results obtained indicate that the finite element analysis based on a suitable constitutive law can appropriately describe the mechanical behaviour of model

tunnel subjected to uniform vertical loading. As to the creep failure test, during the loading stage the numerical results are coincident with the measured, in the creep stage big discrepancy occurred. The Authors conclude that the influence of assuming a plane-strain condition on the prediction of mechanical behaviour of the model tunnel is much larger in creep stage than in loading stage, which should be checked with 3D analysis.

As to the behaviour of tunnels in dynamic condition, due attention has to be paid to the soil-tunnel kinematic interaction, which produces increments of bending moment and hoop force along the transverse section of the lining. The paper presented by *Billotta et al.* shows how successfully centrifuge physical modelling can be employed as benchmark for numerical analyses.

In the centrifuge seismic tests on a circular instrumented aluminium tunnel in dense and loose dry sand performed by the Authors, the adopted instrumentation allowed the soil motion and the internal loads in the lining to be measured. The results were used to calibrate dynamic analyses performed following a pseudo-static uncoupled approach and a full dynamic coupled analysis, in which the soil was modelled as linear visco-elastic (physical modelling results as benchmark for numerical simulations). In Figure 26 are reported the computed and measured peak seismic increments of bending moment, ΔM , and hoop forces, ΔN plotted against the anomaly, θ . Based on the obtained results, the Authors concluded that all the computational methods yielded realistic predictions of the bending moments, while for the hoop forces the scatter between experimental results and the different numerical predictions deserves further investigation.

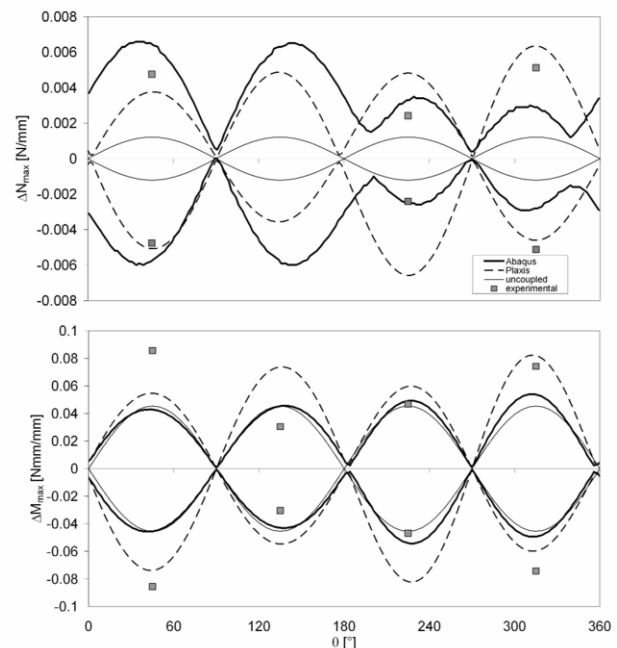


Figure 26. Increments of bending moment M and hoop forces N (EQ2 in model T1, at model scale), from *Billotta et al.*

One of the actual main challenges in underground construction is the developing of widening technique able to minimise the excavation effects on the ground surrounding the tunnel, particularly minimising deformations which could produce huge thrusts on the lining on the final widened tunnel and excessive settlements at the surface. A series of plane strain centrifuge modelling tests have been performed using the ISMGEO centrifuge to simulate the widening of one among two highway tunnels from two to three lanes of the highway A14 nearby Ancona (Italy), designed by the SPEA engineers. A saturated stiff clayey soil was reconstituted from soil sample retrieved from the site around the existing tunnels; miniaturised cone penetration tests have been performed to validate the

mechanical properties of the reconstructed soil; an aluminium alloy lining model was instrumented with strain gauges to monitor the stresses induced by progressive pressure reduction of a membrane which simulates the excavation phase.

The settlements at soil surface and above the crown of the tunnel were measurement by LVDT; pore pressure transducers monitored the soil initial saturation and pore pressure variation induced by excavation. Figure 27 reports the settlement profiles at 4 sections from the soil surface to the invert of the lining model, as measured, in surface by LVDTs and as computed using the image capture technique and analysed by GEOPIV, from the latter the displacement vectors field is shown in Figure 28. Finally Figure 29 reports the pattern of the stresses obtained from the strain gauges internal to the liner model.

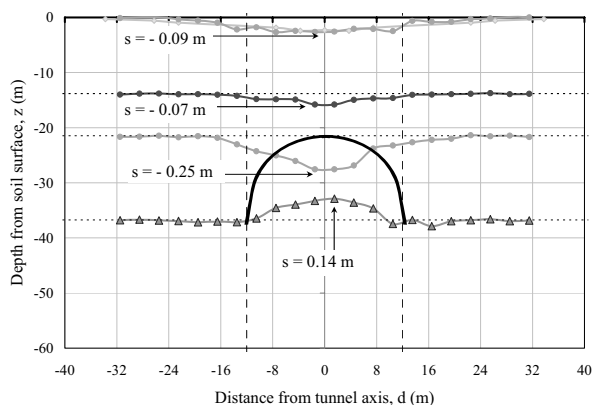


Figure 27. Settlement profiles at 4 sections from the soil surface to the invert of the lining model. From: Collotta et al.

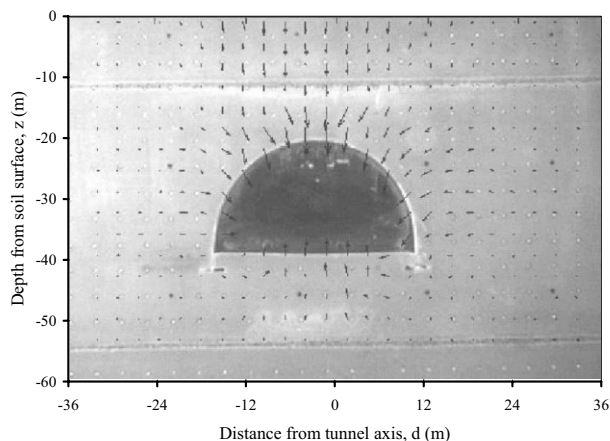


Figure 28. Displacement vectors field. From: Collotta et al.

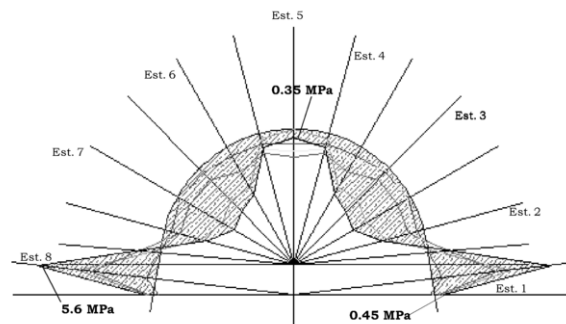


Figure 29. Pattern of the stresses obtained from the strain gauges internal to the liner model. From: Collotta et al.

REFERENCES

- Bonizzoni, F. and Da Prat, M. (2006). Internal Geotechnical Report, Studio Geotecnico Italiano, Milano.
- Boulon, M. and Foray, P. 1986. Physical and numerical simulation of lateral shaft friction along offshore piles in sand. *3rd International Conference on Numerical Methods in Offshore Piling*, Nantes, 127-147.
- Boulon, M. 1988. Numerical and physical modelling of piles behaviour under monotonous and cyclic loading. *Int. Symposium SOWAS '88*, Delft, 285-293.
- Boulon, M. 1989. Basic features of soil-structure interface behaviour. *Computer and Geotechnics* 7, 115-131.
- Burland, J.B. 1987. The Teaching of Soil Mechanics – a Personal View. Proc. 9th European Conference on Soil Mechanics and Foundation Engineering, Dublin, 1, pp.1427-1447.
- Collotta, T., Colognese, S. and Fioravante, V. “Modelling a Highway Tunnel Widening in Stiff Clayey Soil”, to be published.
- Fioravante, V., Giretti D. and Jamiolkowski M.B. (2008a). Physical modelling of piled rafts. *Deep Foundations on Bored and Auger Piles*. Van Impe & Van Impe (eds), pp. 241-248.
- Fioravante, V. 2009. Load Transfer Mechanism Between A Pile And A Raft With An Interposed Granular Layer. Accepted for publication on *Geotechnique*.
- Wernick, E. 1978. Skin friction of cylindrical anchors in non-cohesive soils. *Symposium on Soil Reinforcing and Stabilising Techniques*, Sydney, pp. 201-219.
- Muir Wood, D. 2004. Geotechnical Modelling. *Applied Geotechnics*, Vol. 1. Spon Press, Taylor & Francis Group, London & New York.
- Randolph, M.F. and House, A.R. 2001. The Complementary Roles of Physical and Computational Modelling. *International Journal of Physical Modelling in Geotechnics*, 1, pp. 1-8.